

# ESTAINGIA, A NEW TRILOBITE GENUS FROM THE LOWER CAMBRIAN OF SOUTH AUSTRALIA

by K. J. POCOCK

ABSTRACT. *Estaingia bilobata* gen. et sp. nov. is described from the upper Lower Cambrian Emu Bay Shale of Kangaroo Island, South Australia. The genus resembles the Siberian genera *Lermontovia* Suvorova 1956, and *Bergeroniellus* Lermontova 1940, in the morphology of the cephalon and thorax, but it differs markedly in the structure of the pygidium, which is spinose and bilobed; it has tentatively been placed in the Paradoxididae. The fauna of the Emu Bay Shale also includes new species of *Redlichia* and *Isoxys*, and hyolithids. The palaeoecological implications of the association of *Estaingia* with *Redlichia* are briefly discussed.

IN 1952 Mr. R. C. Sprigg, then of the Geological Survey of South Australia, discovered several richly fossiliferous bands in the Emu Bay Shale at its type locality, between Cape D'Estaing and Emu Bay on the northern coast of Kangaroo Island, South Australia. The main constituent of the fauna is a trilobite which was originally compared with the protolenid *Lusatiops* Richter and Richter (Glaessner, *in* Sprigg 1955), but which is now considered to belong to a new genus.

Subsequent collections have been made by Dr. M. F. Glaessner and Dr. B. Daily of the Department of Geology of the University of Adelaide, members of the staff of the South Australian Museum, and by the author. The fauna is now known to be present at the other known outcrop of the formation, near White Point. Collections from both localities have been studied.

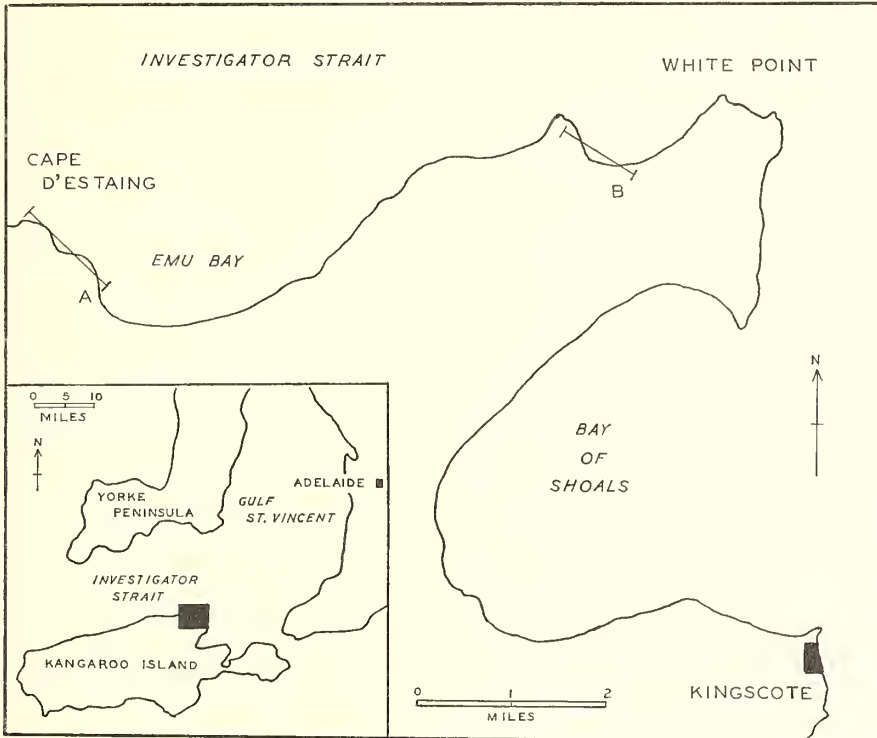
## STRATIGRAPHY

The Emu Bay Shale forms part of the Cambrian succession which outcrops along the northern coast of Kangaroo Island, between Middle River to the west, and Point Marsden to the east (text-fig. 1). General descriptions of the stratigraphy of the area are given by Sprigg (1955), Daily (1956), and Campana (1957). The Emu Bay Shale is known definitely to outcrop at two localities within this area; between Cape D'Estaing and Emu Bay, 9 miles NW. of Kingscote, the type locality, and at 'Big Gully', near White Point, 7 miles NNW. of Kingscote. The formation consists of 300-350 feet of greyish, silty shales, in part fossiliferous, and reddish siltstones with minor arkoses.

At the type locality, the Emu Bay Shale outcrops on the gently dipping, eastern limb of a faulted anticline. It is underlain conformably by the White Point Conglomerate, a rather heterogeneous formation composed of massive conglomerates and interbedded and intertonguing arkoses, with minor shales and mottled limestones. The uppermost bed observed at this locality consists of at least 20 feet of massive arkose, the top of which is obscured. This bed is tentatively correlated with the lowermost bed of the Boxing Bay Formation, which at White Point, conformably overlies the Emu Bay Shale.

Daily (1956, p. 125) has reviewed the evidence for the limits of the age of the White Point Conglomerate, primarily that afforded by fossiliferous boulders found in its conglomerate members. The boulders, containing Archaeocyatha, are attributed to the middle Lower Cambrian Parara Limestone, which outcrops on Yorke Peninsula.

Accordingly, the age of at least part of the White Point Conglomerate is post middle Lower Cambrian. At Emu Bay, a thin band of calcareous shale within mottled limestones, near the top of the formation, contains numerous specimens of an undescribed trilobite. The same genus of trilobite has been previously found on the west side of Cape D'Estaing and at 'Big Gully' in the White Point Section in equivalent beds (Daily 1956, p. 125). However, the affinities and time range of this trilobite are not known, and it cannot be used directly to date the containing beds.

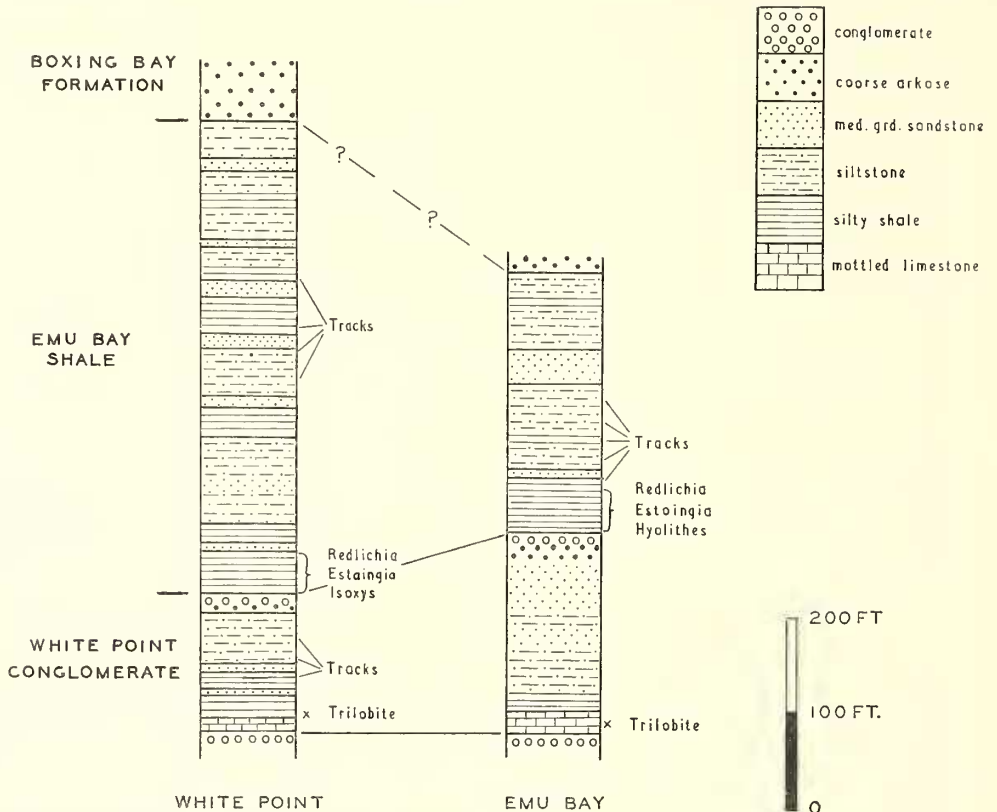


TEXT-FIG. 1. Index map of localities. Inset shows the Emu Bay area (black) in relation to Kangaroo Island and South Australia. A and B show the lines of section through the Emu Bay Shale and White Point Conglomerate, at the two known localities.

The base of the Emu Bay Shale is defined as at the top of the uppermost conglomerate band found in this part of the sequence. The basal beds of the formation consist of 60 feet of dark-grey, silty shales and flagstones, the greater part of which are known to be fossiliferous, containing the trilobites *Estaingia* gen. nov., *Redlichia* sp. nov., a species of *Hyolithes*, a questionable brachiopod, and worm casts; tracks ascribed to trilobites occur higher in the formation. One bed, approximately 2 feet thick, 35 feet from the base of the formation, is richly fossiliferous, but the rest of the zone is only sparingly so.

At White Point the sequence is more complete than at Emu Bay, both boundaries of the Emu Bay Shale being exposed. The last conglomerate band directly referable to the White Point Conglomerate, is conformably overlain by a sequence of dark, silty shales. The basal 40 feet of these shales are richly fossiliferous, containing *Estaingia* gen. nov.,

*Redlichia* sp. nov., *Isoxys* sp. nov., an unidentified crustacean, and annelids. The fossiliferous beds occupy a similar stratigraphic position to those at Emu Bay, and the faunas are basically similar, with the new trilobite *E. bilobata* and the new species of *Redlichia*, as common elements. The correlation of these beds with the basal shales of the Emu Bay Shale in the type section therefore appears justified.



TEXT-FIG. 2. Part of the stratigraphical succession of Cambrian age of Kangaroo Island. 1, White Point section. 2, Type section of Emu Bay Shale, Emu Bay-Cape D'Estaing.

The uppermost beds of the Emu Bay Shale are succeeded by a sequence of approximately 2,000 feet of arkoses and quartzites, with interbedded shales, siltstones, and conglomerates. This sequence, which is unfossiliferous, is known as the Boxing Bay Formation (Daily 1956).

The detailed lithology and thickness of the Emu Bay Shale, and the upper members of the White Point Conglomerate, at both localities, are given in the accompanying stratigraphic columns (text-fig. 2).

#### MODE OF OCCURRENCE AND PALAEOECOLOGY

The fossiliferous rocks of the Emu Bay Shale, at the type locality, are massive, grey, silty shales or fine-grained siltstones; limestone nodules are common throughout, and

the layering has been disrupted by burrowing organisms. The trilobite remains are preserved by replacement of the exoskeletons with calcite, or occasionally iron carbonates. The material consists largely of isolated cranidia and free cheeks, and disarticulated thoracic segments, but some reasonably complete specimens are found, and make up approximately 5 per cent. of the collection. The skeletal elements are unbroken and unabraded and lie mainly, but not entirely, along bedding planes. An extensive size range is represented in the collections of *Estaingia* but although very small holaspids occur, no meraspids or protaspids have been recognized. Many specimens of *Estaingia* show that the cephalon has rolled forward over the detached rostral plate, and that the librigenae are free, but only slightly displaced; this appears to have been the characteristic mode of moulting in this trilobite.

The fossiliferous zone at the White Point locality, consists mostly of dark-grey to black silty shales having a relatively high iron content, in the form of limonite secondarily replacing pyrite, and a high percentage of organic matter; limestone nodules are absent, and the shales are finely laminated. The trilobites are preserved as tests replaced by calcite, but also seem to serve as a locus of deposition for cryptocrystalline haematite. Complete exoskeletons or articulated skeletal elements constitute 80 per cent. of the collection.

It has been noted previously that despite some differences in composition, the faunas at the two localities are basically the same. The relative dominance of the constituents, however, differs; at Emu Bay *Estaingia* and *Hyolithes* are dominant, and *Redlichia* is the minor form, but is persistent throughout the fossiliferous zone; at White Point, *Redlichia* and *Isoxys* dominate the fauna, *Estaingia* is a minor, but again persistent, element, and *Hyolithes* is absent.

The evidence afforded by the lithology of the host rocks, and the preservation of the fossils, suggests that the differences between the faunas from the two localities are due to small variations in the local conditions. The change in environment seems to have been largely chemical. The presence of secondary limonite and haematite (replacing pyrite) and the relatively high percentage of extractible organic matter in the rocks at White Point, indicate that slightly reducing conditions were operative, and suggest restricted circulation and oxygen-poor conditions.

The absence of breakage (except that caused by diagenetic or tectonic processes) and of abrasion, indicates that little or no transport of remains has taken place at either locality. Accordingly at Emu Bay it is probable that the exoskeletons have been secondarily disarticulated and disturbed during the reworking of the sediments by burrowers. At White Point, the reducing environment, at least within the sediment, was inimical to the existence of burrowers and sediment feeders, and the remains consequently escaped disruption.

The available evidence, both sedimentary and palaeontological, points to *Estaingia* having been a benthonic form, perhaps capable of short bursts of swimming, and feeding largely on detritus on the sea floor. *Redlichia*, on the other hand, was probably an efficient swimmer, largely nektonic and predatory in its habits; the presence of tracks referable to it in sediments above and below the fossiliferous zone, however, prove that it spent some of its time crawling on the sea floor. Such a mode of life would render *Redlichia* susceptible to being trapped on the H<sub>2</sub>S poisoned bottom at White Point. *Estaingia*, however, being largely benthonic would venture rarely, and by accident alone, into such an environment. The presence of *Isoxys*, undoubtedly a swimmer, and the complete

absence of *Hyolithes*, a benthonic and probably sessile form, further suggests that the assemblage at White Point accumulated in this manner.

#### METHODS AND TECHNIQUES

The ubiquitous deformation presented many difficulties in reconstruction. The method developed by Henningsmoen (1957) was employed to calculate the true proportions of the cranium, and the reconstruction itself was prepared directly from photographs; the least deformed and best preserved specimens were photographed and these were then enlarged or reduced to a standard size in printing.

Quantitative studies have been carried out on selected samples from the collections, with the aim of supplementing qualitative data on variability and relationships of features of the dorsal exoskeleton, with an accurate statistical description. The methods of analysis of the measurements and their presentation are those recommended by Shaw (1956) and the reader is referred to that paper for a full treatment of the difficulties in dealing with such a sample. On theoretical grounds the method of rectilinear regression is the only valid statistical means for representing variation in most trilobite samples. In the present case this method is not invalidated by the fact that all specimens are deformed in some way, but the results are modified, some of the variation shown being directly attributable to this cause. Despite this fact, the results of the analysis strongly support the hypothesis that the sample comes from a single population, with a rather wide, but continuous range of variation, i.e. a single species. It must be stressed that such an analysis is supplementary, and for this reason, and because comparative data are lacking for most other trilobites studied, a conventional set of measurements on selected specimens, including the holotype, is also included.

#### DESCRIPTION

The specimens are all deposited in the Palaeontological Collection of the University of Adelaide, South Australia (AUGD).

?Family PARADOXIDIDAE Hawle and Corda, 1847

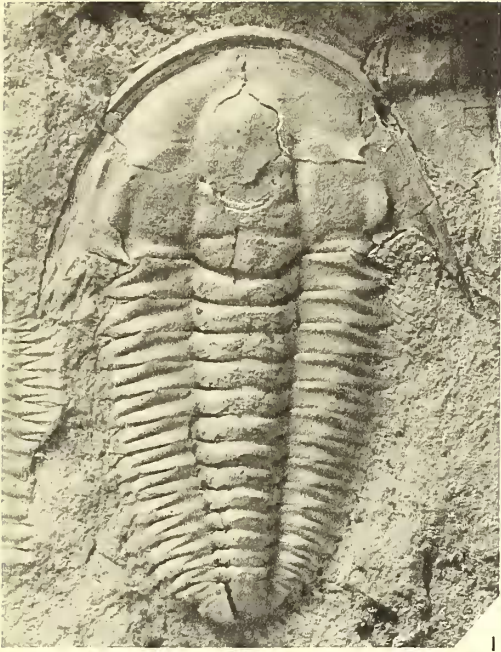
Genus *ESTAINGIA* gen. nov.

Plates 75-76; text-fig. 3

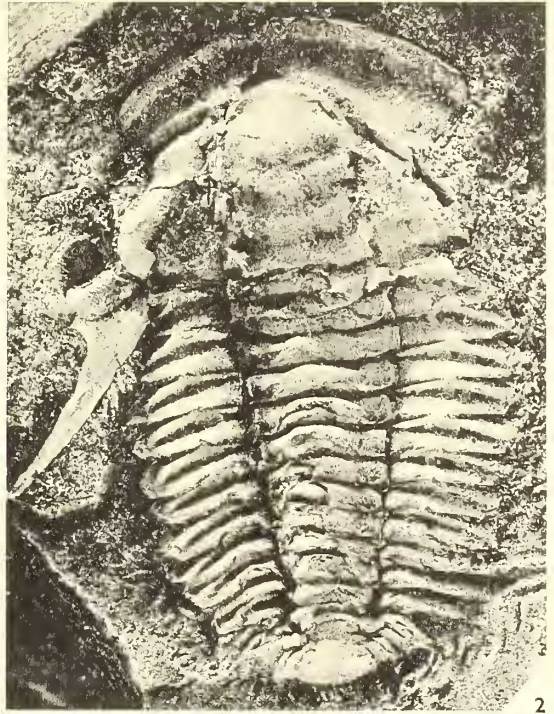
*Derivation of Name.* From Cape D'Estaing, the type locality.

#### EXPLANATION OF PLATE 75

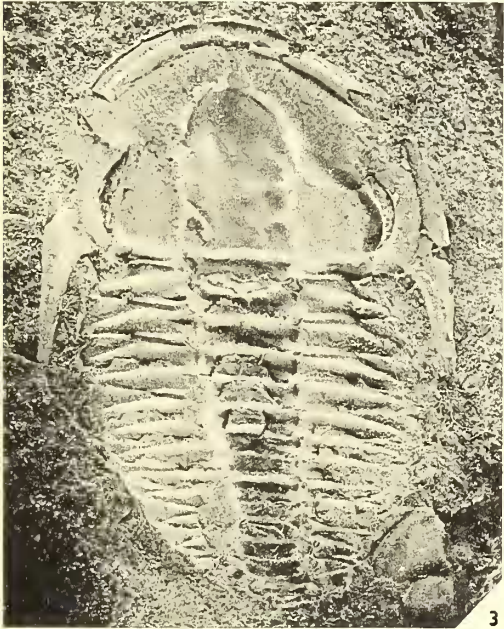
Figs. 1-6. *Estaingia bilobata* gen. et. sp. nov. 1, Holotype AUGD F16441;  $\times 5.5$ . Complete specimen, mould and replaced test. The cranium has rolled forward on the V-shaped rostral plate, flattening it, and disrupting the anterior border. Librigenae displaced and exfoliated, exposing the lateral doublure with terrace lines. The impression of the hypostome is visible under the glabella 2, AUGD F16442;  $\times 4.5$ . Cranium showing impression of rostral plate; glabella deformed. Thorax with 12th segment missing. 3, AUGD F16443;  $\times 3.5$ . Ventral side of disrupted cephalon and fragmentary thorax. Rostral plate *in situ*, damaged. 4, AUGD F16445;  $\times 7$ . Cranium, librigena, and incomplete thorax. 5-6, AUGD F16447;  $\times 6.5$ . Thoracic segment, showing deep apodemal pit, articulating facet, and strong fulcral knob. 6, Rostral plate, complete, showing terrace lines on anterior band.



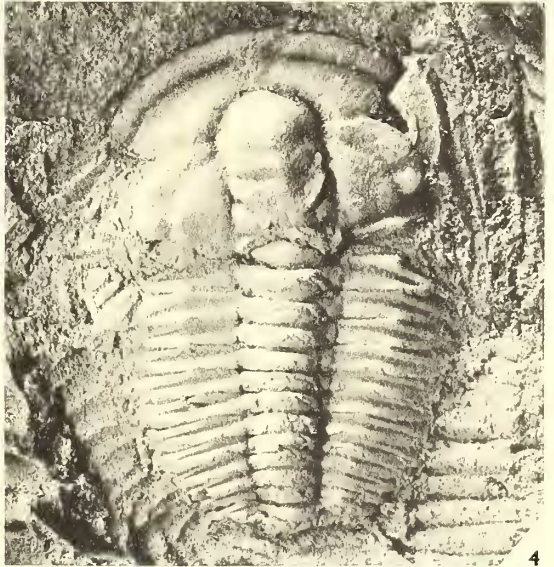
1



2



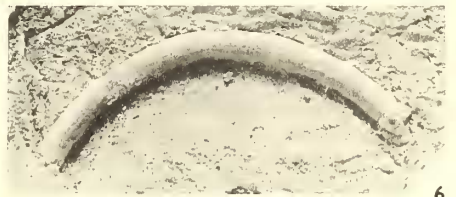
3



4



5

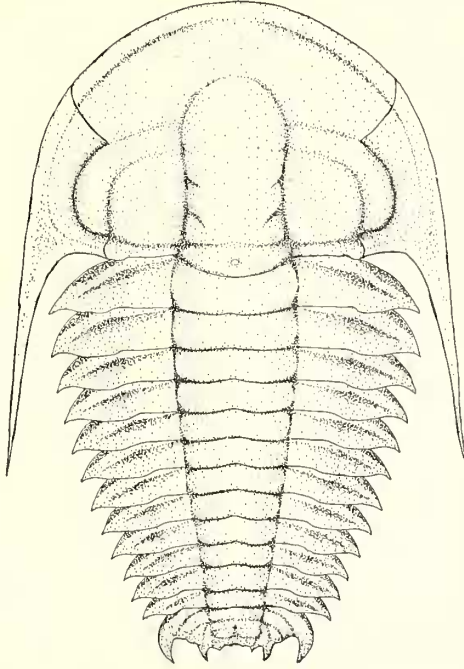


6

POCOCK, Lower Cambrian trilobite



*Diagnosis.* *Estaingia* is a trilobite with protolenid and paradoxidid affinities. Anterior sections of facial sutures diverge at 40–45° to the axis, posterior sections almost parallel to it; functional connective and rostral sutures, free rostral plate slightly shorter than anterior cranidial border; glabella constricted in middle, three pairs lateral glabellar furrows; narrow posterior lateral limb; narrow librigenae with long genal spines. Thorax with twelve segments, pleura falcate, with recurved end, and strong fulcral knob. Pygidium with twelve segments, pleura falcate, with recurved end, and strong fulcral knob. Pygidium



TEXT-FIG. 3. *Estaingia bilobata*. Reconstruction based on specimens illustrated on Plate 75, figs. 1, 5, 6, and Plate 76, figs. 2, 5. Ornamentation and genal caeca here omitted.

small; two segments distinct, one indistinct; wide pleural field, strongly recurved spines; no continuous lateral or posterior border; terminal axial piece bilobed.

*Estaingia bilobata* sp. nov.

Plates 75–76; text-fig. 3

*Derivation of Name.* From bilobed axial part of pygidium.

*Holotype.* AUGD F16441 (Pl. 75, fig. 1); *paratypes*, AUGD F16442–F16550.

*Selection of holotype.* The specimen F16441 was selected as it is the most complete available. The cranidium although damaged shows the distinctive shape of glabella, eye ridges and palpebral lobes, and posterior border and furrow: in addition the impression of the hypostome can be seen on the glabella, and that of the rostral plate just posterior to the anterior border. The librigenae have both been displaced. The spines of the pygidium are missing, but the characteristic segmentation and bilobation are distinct.



*Measurements*: Holotype, F16441. Cephalon: length 6.4 mm.; width (palpebral) 10.0 mm. Cranidium: width (palpebral) 7.2 mm. Librigena: width (palpebral) 1.4 mm.; length (to genal angle) 3.5 mm. Glabella: length 4.1 mm.; width (maximum) 3.0 mm., width (minimum) 2.8 mm. Occipital ring: length 1.0 mm.; width 3.0 mm. Palpebral ridge: width 0.8 mm. Thorax: length 8.0 mm.; width at 3rd thoracic segment (maximum) 8.5 mm.; width axis (at 3rd segment) 2.9 mm. Pygidium: length 1.5 mm.; width (anterior) 5.0 mm.; width (maximum) 5.3 mm.; width of axis (anterior) 1.3 mm. Total length of specimen 15.9 mm.

Cranidium, F16444. Cranidium: length 7.1 mm.; width (palpebral) 9.0 mm.; width (anterior) 8.9 mm. Glabella: length (excluding occipital ring) 4.9 mm.; width (maximum) 3.3 mm.; width (minimum) 2.8 mm. Occipital ring: length 0.5 mm.; width 3.3 mm. Anterior border: width 1.2 mm.

The measurements of various dimensions from selected specimens of the type series and their analysis are presented in Tables 1 and 2, and text-fig. 4.

*Material*. Approximately 200 specimens, generally incomplete, preserved as replaced tests and moulds.

*Occurrence*. Basal 35 ft of the Emu Bay Shale, Kangaroo Island, South Australia. Specimens F16442–F16540 from the type locality of the formation, Cape D'Estaing–Emu Bay, and specimens F16441, F16541–F16550, from the White Point locality. The holotype F16441 is from a bed 15 ft above the base of the formation at Big Gully, near White Point.

*Description*. Cephalon sub-semicircular in outline, moderately convex transversely, gently convex sagittally. Glabella moderately to strongly convex transversely, approximately 3/4 length and 1/4 width of cephalon; slightly constricted at level of middle glabellar furrow, maximum width at level of occipital furrow, and at eye ridge. Three pairs of lateral glabella furrows, all reaching axial furrows abaxially; anterior furrow short, transverse; middle furrow longer, deeper, directed inwards and slightly backwards; pre-occipital furrow long, 1/3 width of glabella, deep, directed inwards and strongly backwards at adaxial end. Pre-occipital and middle glabellar lobe subequal in size; frontal glabellar lobe larger, with outline semicircular to almost wedge-shaped, maximum width at level of anterior edge of eye ridge, strongly convex transversely, gently to moderately convex sagittally, with slight mesial rise continuing back into central area of glabella to level of pre-occipital furrow. Occipital furrow deep behind posterior lobes, swinging forward slightly and becoming shallower sagittally. Occipital ring large, semi-elliptical in shape, maximum width sagittally, decreasing to zero at axial furrows; moderately convex transversely and sagittally; with mesial node. Preglabellar furrow distinct laterally,

---

EXPLANATION OF PLATE 76

Figs. 1–6. *Estaingia bilobata* gen. et. sp. nov. 1, AUGD F16446; ×7. Incomplete cranidium and thorax. Rostral plate visible at top right; posterior border and furrow well developed. Thoracic segments showing deep apodemal pits, strong fulcral knobs, and articulating facets; axis showing distinct change in convexity, adaxial to axial furrow. 2, AUGD F16452; ×7. Librigena, ventral, showing V-shaped lateral doublure. 3, AUGD F16449; ×10. Incomplete pygidium, showing bilobed terminal axial piece, and segmentation of pleural regions. 4, AUGD F16453; ×4.5. Fragment of cranidium on rostral plate, showing well developed genal caeca. 5, AUGD F16444; ×10. Cranidium. 6, AUGD F16448; ×8. Pygidium, external mould.

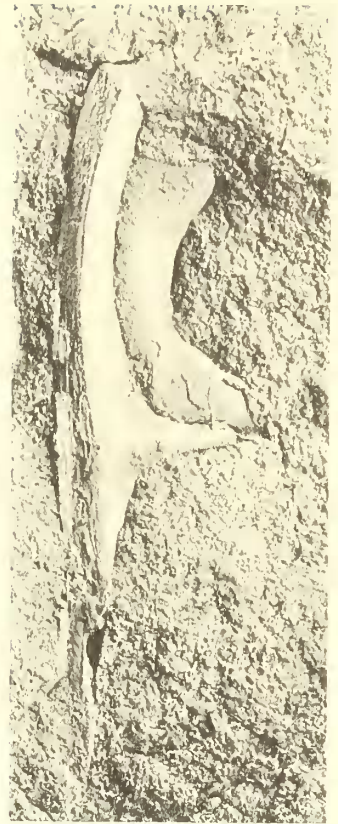
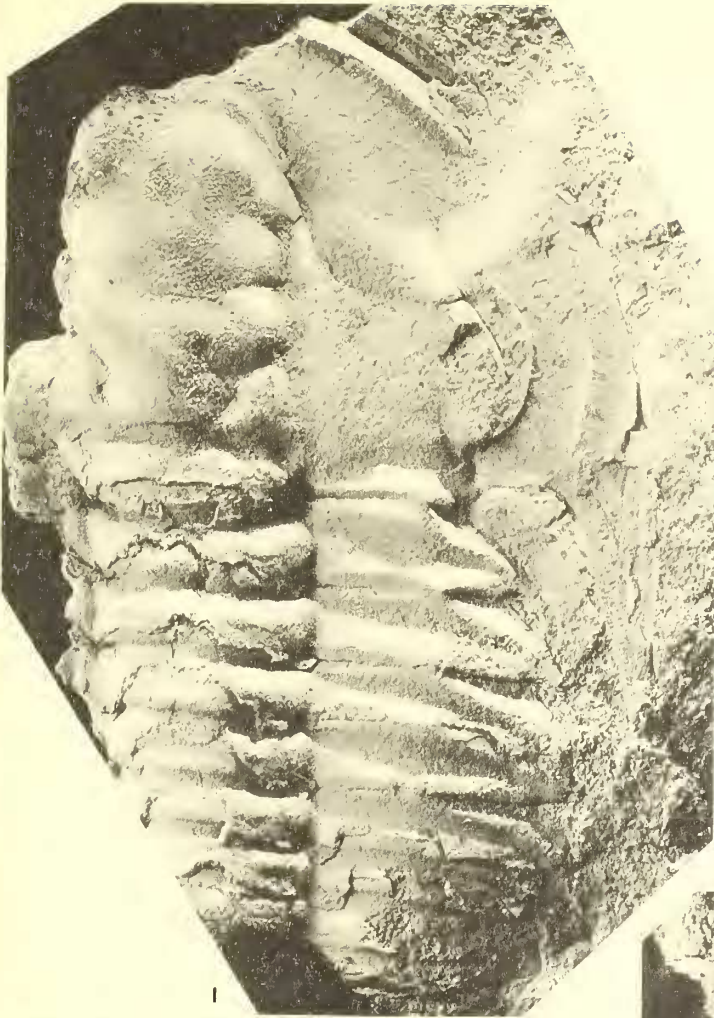




TABLE 1

Selected dimensions of 61 cranidia of *Estaingia bilobata* from Emu Bay, South Australia.  $X$  represents the maximum width of the cranidium,  $Y_1$  the length of the cranidium (exclusive of the occipital ring),  $Y_2$  the maximum width of the glabella, and  $Y_3$  the length of the glabella (exclusive of the occipital ring).

CLASS RANGE X	NO.	DIMENSIONS IN MMS.			
		X	$Y_1$	$Y_2$	$Y_3$
1.5 — 2.4	1	2.0	1.2	0.8	1.0
2.5 — 3.4	1	2.5	1.5	0.8	1.0
3.5 — 4.4	2	3.8	2.8	1.1	1.9
4.5 — 5.4	1	4.2	3.2	1.3	2.1
5.5 — 6.4	1	6.4	5.1	2.3	3.8
6.5 — 7.4	4	6.8	5.3	2.5	3.8
7.5 — 8.4	9	8.0	6.3	3.0	4.4
8.5 — 9.4	9	8.9	6.6	3.3	4.5
9.5 — 10.4	8	9.9	7.4	3.7	5.2
10.5 — 11.4	10	10.9	8.5	4.1	6.0
11.5 — 12.4	6	11.9	9.7	4.4	6.7
12.5 — 13.4	1	12.9	10.8	5.1	7.2
13.5 — 14.4	4	14.1	10.9	5.3	7.7
14.5 — 15.4	3	14.8	11.1	5.2	7.8

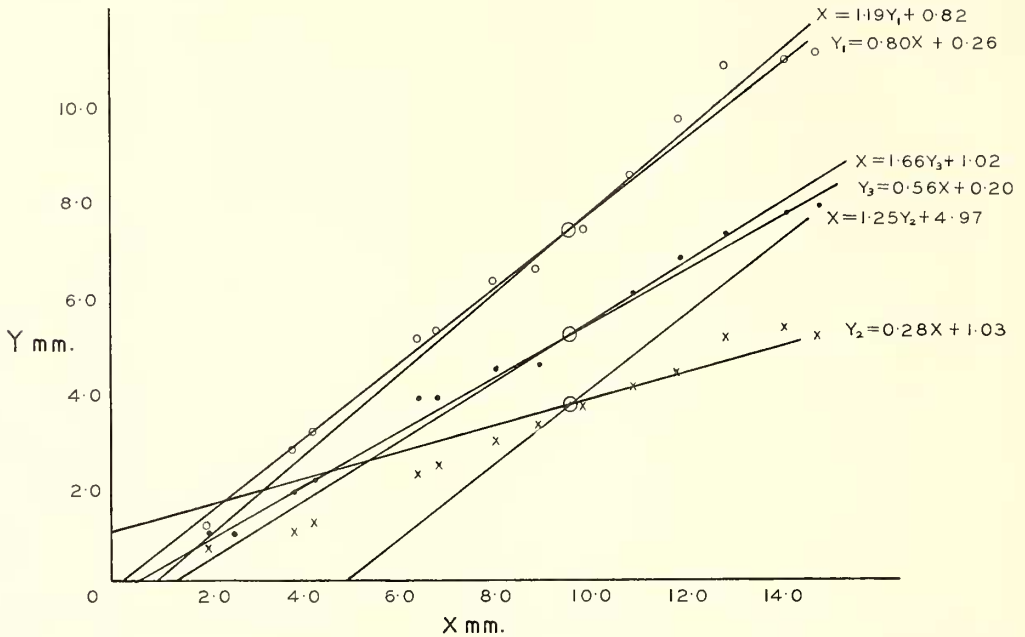
TABLE 2

Analysis of measurements given in Table 1.  $\beta_{xy}$  and  $\beta_{yx}$  are the 95 per cent. confidence intervals for the regression coefficients, respectively, of  $X$  on  $Y$ , and  $Y$  on  $X$ ;  $\alpha_x$  and  $\alpha_y$  are the 95 per cent. confidence intervals for the  $X$  and  $Y$  intercepts.

VARIABLES	COEFFICIENT OF CORRELATION	EQUATIONS OF REGRESSION LINES	$\beta_{xy}$	$\beta_{yx}$	$\alpha_x$	$\alpha_y$
$X - Y_1$	0.97	$Y = 0.80X - 0.26$ $X = 1.19Y + 0.82$	1.15 — 1.26	0.75 — 0.85	0.66 — 1.00	-0.41 — -0.13
$X - Y_2$	0.59	$Y = 0.28X + 1.03$ $X = 1.25Y + 4.97$	0.81 — 1.70	0.18 — 0.38	4.37 — 5.57	0.74 — 1.31
$X - Y_3$	0.96	$Y = 0.56X - 0.20$ $X = 1.66Y + 1.01$	1.54 — 1.78	0.52 — 0.60	0.81 — 1.21	-0.32 — -0.08

becoming indistinct in sagittal line where glabella coalesces with preglabellar field. Preglabellar field gently convex, sloping down from preglabellar furrow and eye ridges to anterior border furrow, transected in some specimens by low, ill-defined, mesial ridge, and crossed by genal caecae. Anterior border furrow well defined exsagittally, shallow and indistinct in position of mesial ridge. Anterior border, slightly elevated, relatively

flat. Genal caecae generally distinct, radiating irregularly from glabella and eye ridges to anterior border furrow causing a slight pitting of the furrow; strong caecae sometimes concentrated in sagittal line, diverging slightly from glabella to border furrow. Palpebral area of fixed cheek subquadrate in shape, slightly depressed centrally. Palpebral lobes broad, moderately to strongly convex, with abaxial side highest, well above general level of free cheek; lobes long, curved, reaching posterior border furrow. Palpebral furrow



TEXT-FIG. 4. Regression analysis of cranial width ( $X$ ) on cranial length ( $Y_1$ ), width of glabella ( $Y_2$ ) and length of glabella ( $Y_3$ ). Data from Table 1. The symbol  $o$  denotes points of the distribution of  $X$  and  $Y_1$ ,  $\bullet$  the distribution of  $X$  and  $Y_3$ , and  $x$  the distribution of  $X$  and  $Y_2$ ; the large circles ( $O$ ) represent the calculated mean for each distribution.

shallow, posterior end distinct, anterior section less distinct. Eye ridges slightly thinner than palpebral lobes, in some specimens separated from them by shallow oblique depressions (possibly a deformational feature), and from glabella by axial furrows; ridges subtransverse, arising just above level of anterior glabellar furrows, posterior sides limited by shallow furrows, anterior sides indistinct, grading into lateral portions of preglabellar field. Posterior lateral limb narrow, short, subtriangular with deep, broad border furrow, and narrow raised border. Posterior border furrow confluent with palpebral furrow and border furrow of librigenae, meeting axial furrows at level just anterior to occipital furrow; deepest abaxially. Posterior border with conspicuous articulating knob toward abaxial end.

Librigenae crescentic, slightly convex transversely, approximately 1/2 width of fixigenae. Border distinct, continuous with genal spine. Ocular surface upsloping from border furrow, sharply upturned at adaxial edge forming narrow eye platform. Genal spines relatively wide at base, narrowing rapidly, and extending at least to level of 8th

thoracic segment. Irregularly radiating genal caecae sometimes observed on ocular surface.

Facial sutures opisthoparian; anterior sections diverge at 40–45° from anterior-lateral corners of palpebral lobes, cross prelabellar field with a slightly sinuous course, then curve inwards across anterior border and become marginal. Posterior sections leave adaxial posterior corners of palpebral lobes, cross posterior border with slightly divergent course. Rostral suture formed by marginal portions of anterior sections of facial sutures; connective sutures cross anterior doublure, separating rostral plate from libriginal doublure; course straight, adaxial to trace of dorsal anterior sutures giving rostral plate shorter than anterior cranial border. Hypostomal suture functional, parallel to rostral suture, possibly as long.

Cranial doublure narrow, marginal rather than ventral. Doublure of librigenae extending inwards to level of border furrow in all positions; V-shaped in cross-section anteriorly, becoming flatter, more rounded towards genal spine; doublure of posterior margin rounded, narrow. Genal spine subtriangular to subrounded in shape. Terrace lines occur on margin of cranium marginal parts of all doublures and on ventral surface of genal spines.

Rostral plate, long, crescentic, forming major part of cranial doublure; width equal to that of anterior border, but shorter than anterior cranial border; V-shaped in cross-section, with narrow marginal strip, downsloping anterior band making 80–100° with upsloping posterior band; anterior portions with terrace lines.

Hypostome not fully known, but appears to consist of a wide crescentic anterior plate, a small convex median body, and a relatively narrow, spinose posterior border.

Thorax of twelve segments; approximately 5/8 length of dorsal exoskeleton; maximum width at level of 3rd segment, narrowing rapidly from 5th. Axis 1/3 width of thorax, markedly convex, but with narrow marginal portions relatively depressed. Axial rings narrow and relatively convex sagittally. Articulating half rings crescent-shaped, moderately convex (sag. and tr.), narrower than axial rings. Transverse furrows deepest laterally, swinging forward slightly and becoming shallow and broad medially. Axial furrows deepest at junction with transverse furrows, shallow opposite axial rings. Apodemal pits present at abaxial end of transverse furrows; marked on ventral side by distinct transverse ridges connected (sagittally) by slightly raised concave platforms. Small axial notch, but no well-developed axial process. Pleura geniculate, with large, but unspecialized fulcral knob. Posterior and anterior margins of adaxial portions of pleura, with narrow overlapping flanges. Abaxial portions with articulating facet, downsloping at 35–40°, particularly well developed on 1st thoracic segment. Distal extremity with small recurved hook, becoming more advanced and less pronounced in posterior segments. Course of pleural furrow obliquely backwards, widening and deepening across fulcrum.

Pygidium sub-semicircular in shape, length (sag.) less than 1/2 maximum width and 1/14–1/16 length of dorsal exoskeleton. Axis 1/3 maximum width, strongly convex, showing traces of two, probably three, segments; posterior half highly vaulted, bilobed with distinct median depression. Pleural regions wide, distinctly segmented, with depressed spinose border. Anterior segment complete, with articulating half ring, transverse furrow, axial ring, and pleural and inter-pleural furrow; anterior band of pleura separated from axis by distinct notch, and produced abaxially into large recurved spine; small articulating facet present. Second segment also distinct; transverse furrow well marked,